Micro-T Circuit Model for Double and Single Sided Induction Heating Systems

Layth Jameel Buni Qaseer

General and Theoretical Electrical Engineering Department
University of Duisburg-Essen, Bismarckstrasse 81, 47057 Duisburg, Germany
laythqaseer@yahoo.com

Abstract - A method is given for obtaining a phase terminal equivalent circuit, which is useful for the analysis of traveling wave as well as longitudinal flux induction systems for heating thin metal strips. The excitation is transverse to the direction of strip motion and can be realized as a three phase system or a single phase system where the strip could be ferromagnetic or nonmagnetic. First, a general form of the field solution is obtained using transfer matrices. A variable transformation is then made which makes it possible to derive an equivalent circuit for each planar region in the system. By joining the equivalent circuits in cascade, an equivalent circuit for the complete system is obtained. The voltages and currents in the equivalent circuit relate directly to the field quantities within the actual system.

Index Terms - Eddy currents, electromagnetic induction, energy conversion, equivalent circuits, induction heating.

I. INTRODUCTION

Traveling wave induction heating (TWIH) systems, as one of the multi-phase induction heating systems, have particular features which make them attractive to achieve various heating applications. Among the advantages are the possibility to heat, quite uniformly, thin strips without moving the inductor above its surface, to reduce the vibration of inductor and load due to electromagnetic forces and, also, the noise provoked by them, to obtain nearly balanced distributions of power and temperature, mechanical strength and the protection for the coils given by the ferromagnetic core [1-7]. The finite element method (FEM) is the most popular numerical method for the analysis of such systems and has been developed in 2-D and 3-D [2-4], [7-10]. Analytical solutions were almost exclusive to cylindrical induction heating systems [5-6], [11-14]. The layer theory approach is an analytical solution of the field problem applied to flat linear machines [15, 16] and cylindrical machines [17-19].

The aim of this paper is to show how the analytical solution to the field problem may be extended to yield an equivalent circuit representation for the induction heating systems.

It is usually straightforward to relate field quantities in the system to voltages and currents in the equivalent circuits. The approach in this paper is presented along a simple multi-region model.

A region in the system is defined by its uniform material in nature having boundaries of simple planar shape.

The equivalent circuits developed here seem to have the form of a cascade of cells made of lumped elements; hence it is possible to consider any number of regions.

The accuracy of the method is verified with measurements of practical induction heating systems, together with comparisons to numerical and analytical methods.

II. MATHEMATICAL MODEL

A general multi-region problem is analyzed. Figure 1 shows a cross section of the *N*-region model used in the theory. The model is taken to be an asset of infinitely long planar regions. The current sheet lies between regions r and r+1. The current sheet varies sinusoidally in the y-direction and with time. It is of infinite extent in the x-

direction and infinitesimally thin in the z-direction.

Regions *1-N* are layers of materials where the general region has a conductivity σ_n and relative permeability μ_n. It is further assumed that

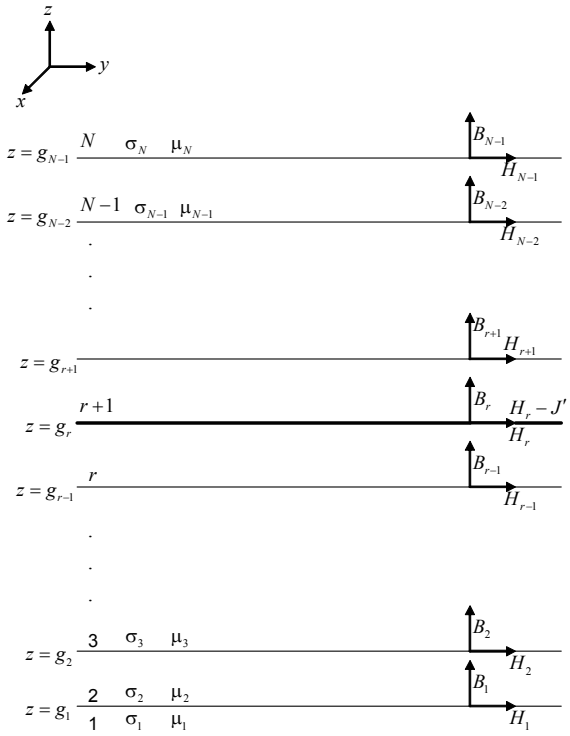

Fig. 1. Cross-section through cylindrical multi-layer induction heating system.

displacement currents at the working frequencies used (from main frequency to several kilohertz) are negligible [15-17] and magnetic materials are assumed linear.

The important field quantities are those acting at the region boundaries. For the models considered here, there are, at most, three field quantities that are relevant. These are the electric field strength E_x which is directed along the interface transverse to the direction of strip motion, the magnetic field strength H_y which is directed axially along the interface and the third one (if existing) is the flux density B_z normal to the interface. If these quantities are known, the equivalent circuit is then derived to obtain the important induction heating system parameters which are the terminal impedance, induced power and axial force.

The intermediate stage between the field solution and the final equivalent circuit is represented in a transmission line form. It is well known that the B_z and H_y values on either side of a region could be linked by a transfer matrix [17]. Hence, every bounded region in the model shown in Fig. 1 could be represented by a corresponding transfer matrix equation.

Figures 2 and 3 show the general outline of a double sided and a single sided induction heating system respectively.

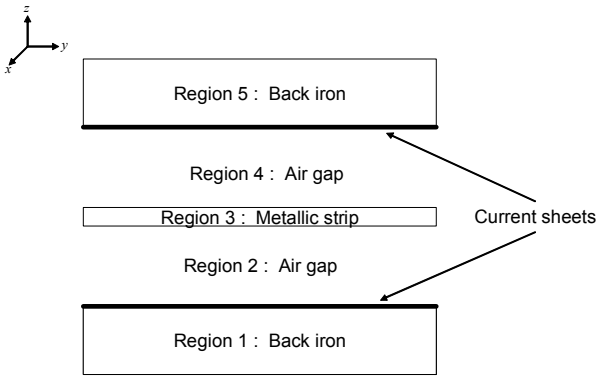

Fig. 2. General outline of a double sided induction heating system.

In the following sections, the theoretical analysis for three phase and single phase excitations are derived.

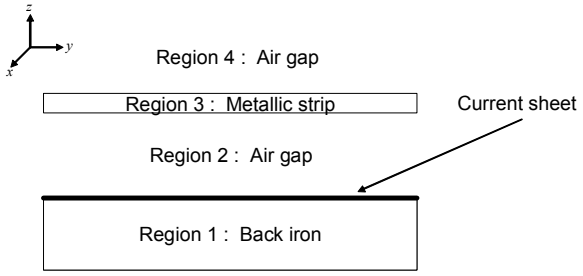

Fig. 3. General outline of a single sided induction heating system.

III. THEORETICAL ANALYSIS

It is assumed that the winding produces a perfect sinusoidal traveling wave. The line current density may be represented as

$$J = \mathrm{Re}\left[J' \exp\left\{ j(\omega t - ky) \right\} \right],$$

where J', ω and k are the amplitude of line

current density, angular frequency and wavelength factor respectively where the latter is related to the pole pitch τ by

$$k = \pi / \tau.$$

A. Field theory solution

The field produced will link all regions from *1* to *N*. Maxwell's equations are solved accordingly to yield (for regions $1 < n < N$)

$$\begin{bmatrix} B_{z,n} \\ H_{y,n} \end{bmatrix} = [T_n] \cdot \begin{bmatrix} B_{z,n-1} \\ H_{y,n-1} \end{bmatrix}, \tag{1}$$

where $B_{z,n}$ and $H_{y,n}$ are the field components at the outer boundary of region n and $B_{y,n-1}$ and $H_{z,n-1}$ are the equivalent values at the inner boundary of the same region and $[T_n]$ is the associated transfer matrix which is given by

$$[T_n] = \begin{bmatrix} \cosh(\alpha_n S_n) & \dfrac{\sinh(\alpha_n S_n)}{\beta_n} \\ \beta_n \sinh(\alpha_n S_n) & \cosh(\alpha_n S_n) \end{bmatrix}, \tag{2}$$

where S_n and α_n are the thickness and attenuation constant of region n, and

$$\beta_n = \frac{\alpha_n}{j\mu_0\mu_n k}.$$

Hence given the values of B_z and H_y at the lower boundary of a region, the values of B_z and H_y at the outer boundary are immediately obtainable from this simple transfer matrix relation. At the boundaries where no excitation current sheet exists, B_z and H_y are continuous; thus for example, if two regions are considered with no current sheet at the common boundary, knowing $B_{z,n}$ and $H_{y,n}$, the lower boundary of the first region, B_z and H_y at the upper boundary of the second region can be calculated by successive use of the underlying two transfer matrices. Considering the current sheet to be at $z = g$, then

$$H'_{y,n} = H_{y,n} \qquad , n \neq r,$$

and

$$H'_{y,n} = H_{y,n} - J' \quad , n = r, \tag{3}$$

where $H_{y,n}$ is the axial magnetic field strength in close lower proximity to the boundary and $H'_{y,n}$ is the axial magnetic field strength in close upper proximity to the boundary.

Given the current sheet excitation at $z = g_r$, the overall structure divides into an upper part, which is modeled according to

$$\begin{bmatrix} B_{z,n-1} \\ H_{y,n-1} \end{bmatrix} = [T_{n-1}] \cdot [T_{n-2}] \cdots [T_{r+1}] \cdot \begin{bmatrix} B_{Z,r} \\ H_{y,r} - J' \end{bmatrix}, \tag{4}$$

and a lower part which supports the following relation

$$\begin{bmatrix} B_{z,r} \\ H_{y,r} \end{bmatrix} = [T_r] \cdot [T_{r-1}] \cdots [T_2] \cdot \begin{bmatrix} B_{z,1} \\ H_{y,1} \end{bmatrix}. \tag{5}$$

Enough information is now available to find all field components; hence, the equivalent circuit model can be set up using the surface impedances of the regions under consideration.

B. Surface impedance calculations

Looking outwards from the current sheet, the surface impedance at a boundary of $z = g$ is defined as [14]

$$Z_{n+1} = \frac{E_{x,n}}{H_{y,n}} = -\frac{\omega}{k} \cdot \frac{B_{z,n}}{H_{y,n}}. \tag{6}$$

And the surface impedance looking inwards is defined as

$$Z_n = -\frac{E_{x,n}}{H_{y,n}} = \frac{\omega}{k} \cdot \frac{B_{z,n}}{H_{y,n}}. \tag{7}$$

Using the method obtained in [14] with the values of $B_{z,N-1}$, $H_{y,N-1}$, B_{z1}, H_{y1} and $[T_n]$ as derived in the previous section then

$$Z_{in} = \frac{Z_r Z_{r+1}}{Z_r + Z_{r+1}}, \tag{8}$$

where Z_{in} is the input surface impedance at the

current sheet and Z_{g+1} and Z_g are the surface impedances looking outwards and inwards at the current sheet. Substituting for Z_r and Z_{r+1} using (7) and (6), respectively, and rearranging the terms yields

$$Z_{in} = -\frac{E_{x,r}}{H_{y,r} - H'_{y,r}}. \quad (9)$$

Substituting (3) into (9) yields

$$Z_{in} = \frac{E_{x,r}}{J'}. \quad (10)$$

From this, the input surface impedance at the current sheet can be determined. All the field components can be found by a straightforward use of this and (7), (4) and (5).

Having found E_x, B_z and H_y at all boundaries, it is then a simple matter to calculate the power entering a region through the concept of the Poynting vector. The time-average power density passing through a surface is usually given as

$$P = \frac{1}{2}\mathrm{Re}\{\bar{E} \times \bar{H}^*\} \quad \mathrm{W}/m^2.$$

Hence the time average power density flowing upwards from the current sheet at $z = g_r$ is given by

$$P'_{in,r} = \frac{1}{2}\mathrm{Re}\left\{E_{x,r} H'^{\,*}_{y,r}\right\},$$

and the time average power density flowing downwards from the current sheet at $z = g_r$ is given by

$$P_{in,r} = -\frac{1}{2}\mathrm{Re}\left\{E_{x,r} H^{*}_{y,r}\right\}.$$

The net power density in a region is the difference between the power in and power out, where

$$P_{in} = -\frac{\omega}{2k}\mathrm{Re}\left\{B_{z,r} H'^{\,*}_{y,r} - B_{z,r} H_{y,r}\right\}. \quad (11)$$

It follows that the tangential force density $F_{y,}$ acting on the strip, is the net power density induced divided by traveling wave velocity $2\tau f$ [15]

$$F_y = \frac{P_{in}}{\lambda f} \quad \mathrm{N}/m^2, \quad (12)$$

where f is the operating frequency.

As the transfer matrix formalism is strictly rooted in the analytical field solutions, the presented formalism might be regarded as sufficient in itself. However, from the technical view point it is hardly possible to draw a clear picture that refers to any of the intended functionalities. Engineers, for the most part, prefer to think in terms of an equivalent circuit model rather than to refer to full-wave time varying field analysis. In addition, the impact of altering design parameters is easier to grasp than in the framework of an applied electromagnetics analysis. For this reason an equivalent circuit model has been developed in the following section.

C. The micro-T terminal equivalent circuit

The underlying transmission-line form of (3)-(5) suggests that, by analogy, some form of equivalent circuit is possible [15]. No loss of generality occurs if only one region is considered. The electric and magnetic field quantities are linked as shown in (1) and by making use of the relation

$$E_x = -\frac{\omega}{k} \cdot B_z.$$

In order to represent the relationship between E_n, H_n and E_{n-1}, H_{n-1} by a corresponding T-circuit, a change of variable is required. Without such a transformation it does not appear to be possible to represent a region with such a simple 3-element circuit. Engineers prefer to think in terms of an equivalent circuit rather than time varying field problem as represented in [20, 21]. A practical variable transformation refers to the variable *E*, which is changed to *wE,* where *w* is the width of the strip.

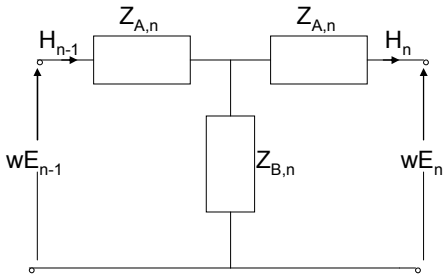

Fig. 4. Basic T-circuit for region *n*.

A T-circuit can now be used to link the variables *wE* and *H* on either side of a region as shown in Fig. 4.

In effect, the current H_n in a T-circuit is driven by a voltage wE_n. For the general region *n*, the impedances are given by the following relations [17]

$$Z_{A,n} = Z_n' \tanh(\frac{\alpha_n S_n}{2}) \tag{13}$$

$$Z_{B,n} = \frac{Z_n'}{\sinh(\alpha_n S_n)}, \tag{14}$$

where Z_n' is the characteristic impedance of region *n* and is defined by the relation

$$Z_n' = \frac{j\omega\mu_0\mu_n}{\alpha_n}, \tag{15}$$

where μ_n is the relative permeability of region n. The attenuation constant α_n is defined by

$$\alpha_n = (k^2 + j\omega\sigma_n\mu_0\mu_n)^{\frac{1}{2}},$$

where σ_n is the conductivity of region n.

As a check, if this circuit is loaded with an impedance Z_{n+1}, the input impedance is Z_n as given in (7). Regions *2* to *N-1* in the general case could all be replaced by such circuits. Regions *1* and *N* would simply require a single impedance which is the characteristic impedance of the respective region as in (15).

On joining the T-circuits in cascade, the full basic equivalent circuit for the single sided traveling wave induction heating system is obtained as shown in Fig. 5.

For DSIH systems, the full basic equivalent circuit is shown in Fig. 6.

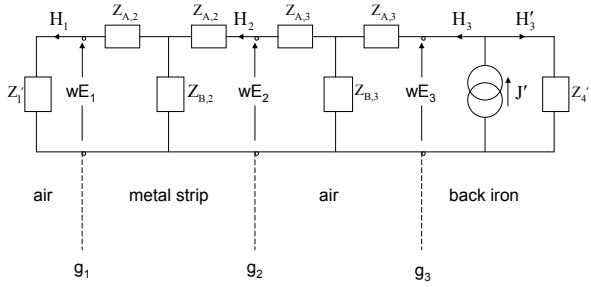

Fig. 5. Basic equivalent circuit for a single sided induction heating system.

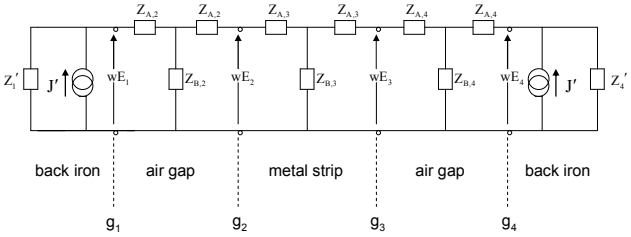

Fig. 6. Basic equivalent circuit for a double sided induction heating system.

Thus an equivalent circuit has been derived by a rearrangement of the field solution, where the voltages and currents are directly related to the field quantities.

It is convenient to think in terms of phase voltages and currents. The input quantities to the basic equivalent circuit are the current J' and the voltage wE_r. The relation between J' and the r.m.s. phase current *I* can be written as

$$J' = \frac{6\sqrt{2}N_{eff}I}{\tau p},$$

where *p* is the number of poles and N_{eff} stands for the effective number of series turns per phase, hence

$$I = (I_{fac})J', \tag{16}$$

where

$$I_{fac} = \frac{\tau p}{6\sqrt{2}N_{eff}},$$

The phase voltage is linked to wE_r by

$$V = \sqrt{2}N_{eff}wE_r, \quad (17)$$

therefore,

$$V = V_{fac}wE_r, \quad (18)$$

where

$$V_{fac} = \sqrt{2}N_{eff}.$$

Let us now consider the effect of multiplying the quantities wE_n and H_n terms in the basic equivalent circuit by the factors V_{fac} and I_{fac} respectively then, the impedances in the basic circuit have to be multiplied by an impedance factor given by

$$Z_{fac} = \frac{V_{fac}}{I_{fac}} = \frac{12(N_{eff})^2}{\tau p}, \quad (19)$$

and the terminal impedance of the induction heating system is given by

$$Z_t = Z_{fac}wZ_{in} \quad \Omega. \quad (20)$$

This relation results in a completely new equivalent circuit in which the input quantities are the r.m.s voltage and r.m.s. current using (18) and (16). Thus the various voltages and currents at the input to each T-circuit are now related directly to the field quantities at the corresponding interfaces of the induction heating system and this terminal equivalent circuit has all the advantages of the basic circuit but, in addition, the impedances are real impedances.

IV. NUMERICAL RESULTS

The equivalent circuit method that has been described in the previous section is validated through a numerical example. Reference [7] employed a double sided induction heating system whose data are given in Table 1. Five regions are required to simulate a double sided system, therefore three T-circuits are combined together and terminated by characteristic impedances of outer regions which are the backing iron regions as shown in Fig. 3.

For comparison reasons, FEM computation is adopted in our analysis which is widely used as a numerical technique for this kind of applications.

In our implementation, the field domain is divided into a number of regions, each being defined by its coordinates, permeability and conductivity. Each region is descritized using first order triangular elements [22]. The induced power in the charge is obtained through the solution of governing differential equation for each nodal magnetic vector potential. Three values of power are computed: the power integrated over the coil, the air gap power and the power integrated over the charge.

Table 1. Problem data for traveling wave dish and ssih systems [9].

Strip thickness, (mm)	2
Strip width, (mm)	1000
Strip length, (mm)	960
Relative permeability of strip	1
Mean strip conductivity, (S/m)	3.03×10^7
Axial pole pitch, (mm)	480
Slot pitch, (mm)	160
Slot width, (mm)	80
Slot depth, (mm)	40
Slots per pole per phase	1
Number of axial poles	2
Number of conductors per slot	8
Frequency, (Hz)	50
Inductor axial length, (mm)	960
Inductor width, (mm)	1000
Magnetic yoke depth, (mm)	80
Air gap length between yoke & strip, (mm)	15
Amplitude of line current density, (kA/m)	200
Input phase voltage, (V)	220

The solution is assumed to be convergent when these three values do not differ by more than 1% which is termed as the power mismatch or power

imbalance.

For the sake of comparison, the same model is adopted as a single sided induction heating system using the same line current density by removing one of the inductors along with its backing iron. Four regions are required to simulate a single sided system therefore two T-circuits are combined together and terminated by characteristic impedances of outer regions which are the backing iron region and outer air region as shown in fig.4.

Table 2 shows the computed parameters for both systems using FEM and the micro-T circuit model. Results obtained using both methods are in good agreement as shown in Table 2. This agreement is attributed to the fact that strip thickness is very small compared to strip length and width which coincides with the assumptions made in the mathematical model.

Table 2. Computed parameters for traveling wave induction heating systems.

Parameter	FEM value	Layer Theory value
Per phase DSIH strip resistance (Ω)	0.0497	0.0513
Per phase DSIH reactance (Ω)	0.014	0.017
DSIH strip power (kW)	1210.3	1250.2
DSIH axial force (N)	23914.5	26045.3
Per phase SSIH strip resistance (Ω)		0.0125
0.012		
Per phase SSIH reactance (Ω)	0.0087	0.0086
SSIH strip power (kW)	305.06	292.8
SSIH axial force (N)	6300	6099.9

Figures 7 and 8 show respectively the variation of normal and tangential (axial) flux density components (B_z, B_y) along magnetic gap length. The maximum deviation between the results of both methods is found to be 5.2%.

Figures 9 and 10 show the variation of normal and tangential (axial) flux density components (B_z, B_y) along distance normal to the strip. Again both methods correlate well within 4%. In both systems, the axial flux density component in the air gap is greater than the normal component, this may be attributed to the fact that the pole pitch is much greater than the air gap length in both systems and in this case these systems are considered as axial flux machines. It is clear from these figures that the axial component of magnetic flux density is decreased within the strip due to skin effect which is not effectively pronounced in the normal component to the strip.

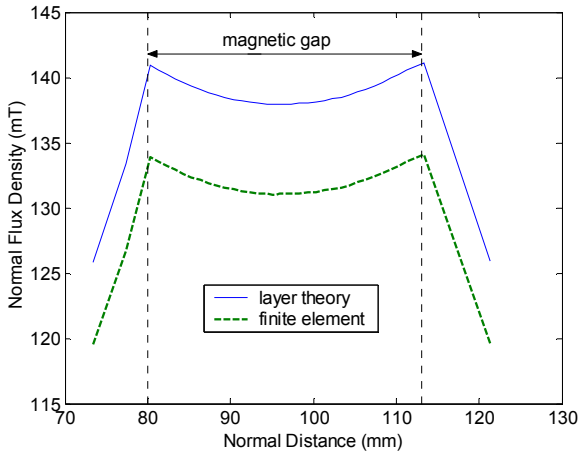

Fig. 7. Variation of normal flux density component along normal distance to strip for double sided induction heating system.

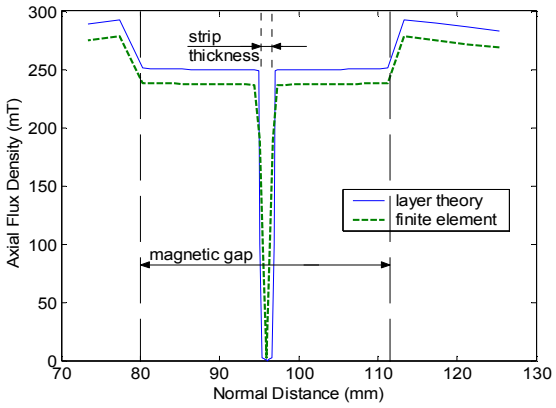

Fig. 8. Variation of axial flux density component along normal distance to strip for double sided induction heating system.

It should be appreciated that comparisons of computed field values in multilayer simulation problem of electrical machines with real field data are found in literature [18, 23].

V. CONCLUSION

The micro-T circuit has been used for the analysis of single and double sided traveling wave induction heating systems. It can be used for any number of regions, and with any number of poles. Using such circuits may provide a better technical

insight into the system than is possible from studying the full-wave solutions from a computational electromagnetics analysis.

Given just the voltages and currents in the terminal equivalent circuit, the field quantities at any region boundary can be easily derived. The obtained results agree well with the data from the corresponding FEM analysis.

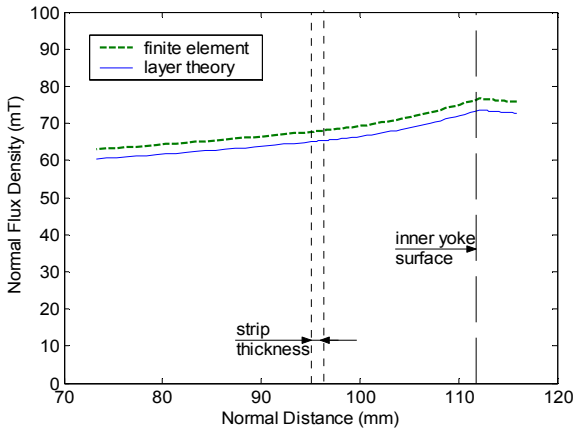

Fig. 9. Variation of normal flux density component along normal distance to strip for single sided induction heating system.

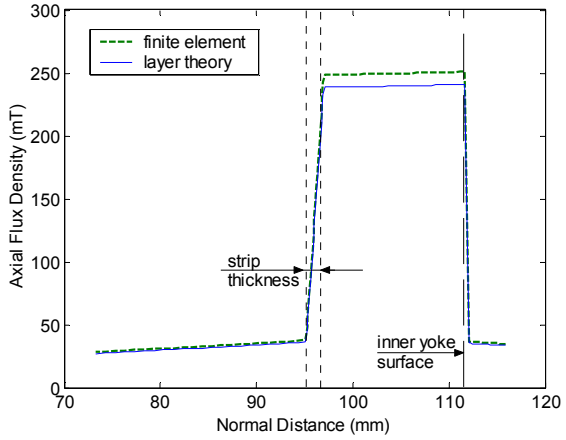

Fig. 10. Variation of axial flux density component along normal distance to strip for single sided induction heating system.

ACKNOWLEDGMENT

The author is deeply indebted to Professor Daniel Erni, his host and co-worker at the University of Duisburg-Essen for advice and encouragement. This work was supported in part by the DAAD under Grant A0901170.

REFERENCES

[1] W. Jackson, “Analysis of edge effects in traveling wave inductors heating metal products,” *Proc. Of NCE-UIC Electroheat for Metals Conf.*, vol. 5, no. 3, 1982.

[2] S. Lupi, M. Forzan, F. Dughiero, and A. Zenkov, “Comparison of edge-effects of transverse flux and traveling wave induction heating inductors,” *IEEE Trans. Magn.,* vol. 35, no. 5, pp. 3556-58, 1999.

[3] L. Pang, Y. Wang, and T. Chen, “Analysis of eddy current density distribution in slotless traveling wave inductor,” *Proc. ICEMS*, pp. 2865-68, 1998.

[4] J. Wang, J. Li, Y. Wang, and X. Yang, “Simulation of traveling wave induction heating systems,” *Proc. WAC World Automation Conf.*, pp. 1-4, 2008.

[5] V. Bukanin, F. Dughiero, S. Lupi and V. Nemkov, "Simulation and design problems of multiphase induction heating systems", *Proc. 37th Int. Wiss Kolloquium,* pp. 588-593, 1992**.**

[6] V. Vadher, "Theory and design of traveling wave induction heaters," *Proc. BNCE-UIE Electroheat for Metals Conf.*, vol. 5, no. 1, 1982.

[7] F. Dughiero, S. Lupi, V. Nemkov, and P. Siega, “Traveling wave inductors for the continuous induction heating of metal strips,” *Proc. Mediterranean Electrotechnical Conf.*, pp. 1154-1157, 1994.

[8] L. Pang, Y. Wang, and T. Chen, “Analysis of eddy current density distribution in slotless traveling wave inductor,” *Proc. ICEMS*, pp. 2865-68, 1998.

[9] Y. Wang and J. Wang, “The study of two novel induction heating technology,” *Proc. ICEMS, conf.*, pp. 572-574, 2008.

[10] S. Ho, J. Wang, W. Fu, and Y. Wang, “A novel crossed traveling wave induction heating system and finite element analysis of eddy current and temperature distributions,” *IEEE*

Trans. Magn., vol. 45, no.10, pp. 4777-80, 2009.

[11] A. Ali, V. Bukanin, F. Dughiero, S. Lupi, V. Nemkov, and P. Siega, "Simulation of multiphase induction heating systems," *Proc. Computation in Electromagnetics International conf.,* pp. 211-214, 1994.

[12] F. Dughiero, S. Lupi, and P. Siega, "Analytical calculation of traveling wave induction heating systems," *Proc. International Symposium on Electromagnetic Fields in Electrical Engineering*, pp. 207-210, 1993.

[13] V. Vadher and I. Smith, "Traveling wave induction heaters with compensating windings," *Proc. International Symposium on Electromagnetic Fields in Electrical Engineering*, pp. 211-214, 1993.

[14] L. Bunni and K. Altaii, "The layer theory approach applied to induction heating systems with rotational symmetry," *Proc. IEEE Southeast Conf.*, pp. 413-420, 2007.

[15] J. Greig and E. M. Freeman, "Traveling wave problem in electrical machine," *Proc. IEE*, vol. 114, no. 11, pp. 1681-1683, 1967.

[16] E. M. Freeman, "Traveling waves in induction machines: input impedance and equivalent circuits," *Proc. IEE*, vol. 115, no. 12, pp. 1772-1776, Dec. 1968.

[17] E. M. Freeman and B. E. Smith, "Surface impedance method applied to multilayer cylindrical induction devices with circumferential exciting currents," *Proc. IEE*, vol. 117, no. 10, pp. 2012-2013, Oct. 1970.

[18] J. F. Eastham and J. H. Alwash, "Transverse flux tubular motors," *Proc. IEE*., vol. 112, no. 12, pp. 1709-1718, 1972.

[19] J. H. Alwash, A. D. Mohssen, and A. S. Abdi, "Helical motion tubular induction motor," *IEEE Trans. Energy Convers.,* vol. 18, no. 3, pp. 362 – 396, 2003.

[20] E. M. Freeman, "Equivalent circuits from electromagnetic theory: low frequency induction devices," *Proc. IEE*, vol. 121, no. 10, pp. 1117-1121, 1974.

[21] E. M. Freeman and T. G. Bland, "Equivalent circuit of concentric cylindrical conductors in an axial alternating magnetic field," *Proc. IEE*, vol. 123, no. 2, pp. 149-152, 1976.

[22] P. P. Silvester, and R. L. Ferrari, *Finite Elements for Electrical Engineers,* 3rd edition, Cambridge University Press, 1996.

[23] J. H. Alwash, *Analysis and Design of Linear Induction Machines*, Ph.D. thesis, Imperial College, University of London, U.K., 1972.

L. J. B. Qaseer was born in Baghdad, Iraq, on October 14, 1957**.** H**e** received his B.Sc., M. Sc. and Ph.D. degrees from the University of Baghdad in 1979, 1993 and 2004 respectively, all in electrical engineering. In 2005, he was with the Mechatronic Engineering Department at the University of Baghdad. Dr. Qaseer is currently with the General & Theoretical Electrical Engineering Department of the University of Duisburg-Essen, Duisburg, Germany. His special fields of interest include rotary, linear, tubular linear and helical motion induction motors, as well as induction heating.